Volume 2 | Number 12 | December 2015

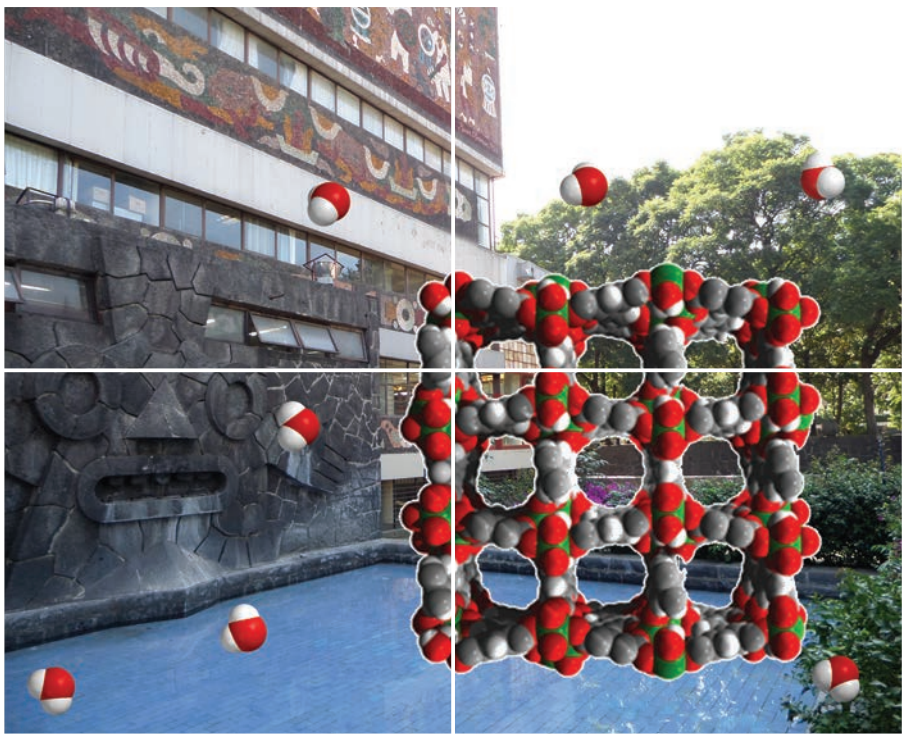

INORGANIC CHEMISTRY

FRONTIERS

Chinese Chemical Society

ROYAL SOCIETY OF CHEMISTRY

http://rsc.li/frontiers-inorganic

INORGANIC CHEMISTRY
FRONTIERS

RESEARCH ARTICLE

Cite this: *Inorg. Chem. Front.*, 2015, **2**, 1091

Cation deficiency effect on negative thermal expansion of ferroelectric $PbTiO_3$†

Xin Peng,[a] Yangchun Rong,[a] Longlong Fan,[a] Kun Lin,[a] He Zhu,[a] Jinxia Deng,[b] Jun Chen[a] and Xianran Xing*[a]

Received 20th August 2015,
Accepted 2nd October 2015

DOI: 10.1039/c5qi00154d

rsc.li/frontiers-inorganic

It is known that negative thermal expansion (NTE) in $PbTiO_3$ (PT) ferroelectrics can be controlled by chemical substitutions. In the present work, however, we report a method to change the NTE of PT by introducing cation deficiency at both the A (Pb^{2+}) and B sites (Ti^{4+}). We investigated the spontaneous polarization, tetragonality *c*/*a*, coefficient of thermal expansion, and Curie temperature T_C with 8% Pb^{2+} deficient PT ($P_{92}T$), 2% Ti^{4+} deficient PT (PT_{98}), and pure PT. We found that while Pb^{2+} deficiency distinctively weakens the NTE, the effect of B-site deficiency could be ignored. These phenomena are ascribed to the NTE mechanism of spontaneous volume ferroelectrostriction. The present study provides a possible way to control the NTE of PT-based materials.

Introduction

It is well known that most materials expand upon heating due to the inherent anharmonicity of bond vibrations. Over the past decades, however, negative thermal expansion (NTE) has been reported in some materials,[1–15] and its discovery has made it possible to reduce thermal shock in various applications. $PbTiO_3$ (PT) is a very popular NTE material featuring spontaneous polarization (P_s) parallel to the polar direction of the *c* axis.[16,17] In our group, the NTE of PT was found in the temperature range of 25–490 °C.[15] Afterward, systematic investigations have been carried out to adjust the NTE in PT-based compounds.[18–22] Chemical substitutions of Pb and Ti cations are used to achieve wide control of the coefficient of thermal expansion (CTE). For example, in the systems of $(1-x)PbTiO_3$–$xBiFeO_3$[18] and $(Pb_{1-x}Cd_x)TiO_3$,[19] chemical substitutions enhanced NTEs, resulting in a CTE of -3.92×10^{-5} °C^{-1} for $x = 0.6$ and -2.40×10^{-5} °C^{-1} for $x = 0.06$ in the corresponding compound. Furthermore, in $(1-x)PbTiO_3$–$xBi(Zn_{1/2}Ti_{1/2})O_3$[20] and $(1-x)PbTiO_3$–$xBi(Ni_{1/2}Ti_{1/2})O_3$,[21] near zero thermal expansions were achieved. Cation doping cripples NTE of PT in most cases. For example, the NTEs of $PbTi_{1-x}Fe_xO_3$ are reduced to -1.49×10^{-5} °C^{-1} and -1.13×10^{-5} °C^{-1} when $x = 0.05$ and 0.10,[22] respectively. All this evidence[16] shows a strong correlation between the spontaneous polarization and NTE for PT-based ferroelectrics, known as spontaneous volume ferroelectrostriction (SVFS), which is a newly identified mechanism in ferroelectric NTE compounds.[23]

To date, the influence of A/B-site deficiency on NTE in $PbTiO_3$ has not been reported. In the present work, we prepared nonstoichiometric PT samples to introduce Pb^{2+}/Ti^{4+} deficiencies. The Pb^{2+}/Ti^{4+} deficiencies can cause a spontaneous polarization displacement change, which in turn causes a distortion of the primitive cell, and thus controls its CTE. The experimental results show that the CTE of PT with 2% Ti^{4+} deficiency (PT_{98}) is nearly equal to that of pure PT, while the NTE of an 8% Pb^{2+} deficient compound ($P_{92}T$) is significantly weakened.

Experimental

Solid solution samples with Pb^{2+}/Ti^{4+} deficiencies were prepared using a conventional solid state reaction route. Analytical reagent grade raw materials of PbO and TiO_2 were weighed in stoichiometric proportions and pestled for an hour in an ethanol medium. The mixed powders were calcined at 850 °C for 5 hours for perovskite phase formation. Then, the solid solution samples were sintered at 900 °C for two hours. In the A-site deficiency experiment, we set $TiO_2 : PbO = 1 : x$, $x < 1$; and in the B-site deficiency testing, we set $PbO : TiO_2 = 1 : x$, $x < 1$. The X-ray diffraction (XRD) patterns of the sintered samples were taken using a laboratory diffractometer (PANalytical X' PertIII, Holland) (Cu Kα radiation). The high-temperature powder X-ray diffraction patterns were collected using the same diffractometer and an Anton Paar HTK 1200 high-temp-

[a]*Department of Physical Chemistry, University of Science and Technology Beijing, Beijing, 100083, P. R. China*
[b]*Department of Chemistry, University of Science and Technology Beijing, Beijing, 100083, P. R. China. E-mail: xing@ustb.edu.cn; Fax: +86 10 6233 2525; Tel: +86 10 62334200*

†Electronic supplementary information (ESI) available. See DOI: 10.1039/c5qi00154d

erature attachment was used. Data were collected from 25–700 °C over a 2θ range from 20 to 80°. The heating rate was 10 °C min^{-1} and the sample was held for 5 min at a specified temperature to reach heating equilibrium. The structure was refined using the Rietveld method using FULLPROF software. The T_C (the temperature where the ferroelectric transforms into a paraelectric one in lead titanate) of these samples was defined using DSC (Labsys Evo, Setaram, France). The heating rate was 10 °C min^{-1} in air conditions and the rate of the airflow was 25 mL min^{-1}. Raman measurements were performed using a LabRAM HR Evolution Raman spectrometer (Jobin Yvon, France). The 532 nm line of an argon ion laser was used as the excitation light. The output power of the laser was kept within 0.4 mW. The compositions of the samples were identified using energy-dispersive spectroscopy (SEM-EDS) (FE-SEM, SUPRA-40, Carl Zeiss) and inductively coupled plasma optical emission spectroscopy (ICPOES; Thermo IRIS Intrepid II). Ion oxidation states in the samples were analyzed using X-ray photoelectron spectroscopy (ESCALAB 250Xi, Thermo Fisher). Experimental details are included in the ESI.†

Results and discussion

PT has a perovskite structure (ABO_3) where large Pb atoms occupy the A-site and small Ti atoms occupy the B-site. It is known that a perovskite structure has a flexible crystal structure that allows cation deficiency at the A/B site. A single perovskite phase can be achieved with various concentrations of A/B site deficiency, and while a larger amount of deficiency can be stabilized at the A site, an impure phase appears when more deficiency is introduced. To study the B-site deficiency of PT, we set $Pb^{2+}:Ti^{4+} = 1:x$. The prepared sample is not in a single phase when $x < 0.98$. Similarly, in the A-site Pb^{2+} deficiency situation with the chemical ratio of $Ti^{4+}:Pb^{2+} = 1:x$, the impurity is detected in the sample with $x < 0.92$. For example, the PbO and $PbTi_3O_7$ impurity phases are detected in the nominal PT_{97} and $P_{91}T$ samples. To study the actual compositions of the prepared samples, SEM-EDS measurements were carried out. The averaged measured results (Table 1) agree well with the nominal compositions (error <5%, the individual ones can be seen in Tables S2–S4 in ESI†). The EDS results of the different areas are close to each other, indicating the compositional homogeneity. Also ICP tests were adopted to confirm the results. The Pb^{2+}/Ti^{4+} ratios from the ICP tests are 1/1.00, 0.94/1 and 1/0.97 for PT, $P_{92}T$ and PT_{98}, respectively, confirming the EDS measurements. In addition, the XPS results reveal that the valence states of the Ti^{4+} and Pb^{2+} ions exist only, while oxygen vacancies increase with more introduced cations (Fig. S4 and S5 in ESI†). These results show that a large amount of deficiencies can be stabilized at the A-site but not in the B-site. We know that the TiO_6 octahedron is the framework of the perovskite structure of $PbTiO_3$ and the Pb atom is in the cave of the framework, surrounded by twelve oxygen atoms to form a PbO_{12} polyhedron. We can thus reasonably speculate that this is why the amount of Pb^{2+} deficiency could be much bigger than the Ti^{4+} deficiency in single phase PT.

As shown in Fig. 1, PT_{98} and $P_{92}T$ samples are in pure tetragonal phases, and the crystal structure can be well refined using the same structure model with PT (*P4mm*). In Table 1, we compare the *c*/*a*, cell volume, P_s at room temperature and T_C of $P_{92}T$, PT_{98} and PT. It is found that PT and PT_{98} are very similar in their structural properties, whereas $P_{92}T$ is greatly different from PT. The *c* axis of $P_{92}T$ is also smaller than that of PT, while the *a* axis is bigger than that of PT. Thus, the *c*/*a* of $P_{92}T$ (1.060) is smaller than that of PT which has a value of 1.065. The unit cell volume of $P_{92}T$ at room temperature is also smaller than that of PT. It is known that the ferroelectric dipole is aligned with the direction of the *c* axis, which strongly correlates with the lattice and the P_s displacement. As shown in Table 1, the A-site P_s displacement of $Pb^{2+}(\delta z_{Pb})$ decreases from 0.524 Å of PT to 0.497 Å of $P_{92}T$, while the B-site P_s displacement of $Ti^{4+}(\delta z_{Ti})$ decreases from 0.400 Å to 0.368 Å. This indicates that the reduction in the *c* axis is due to its close relation with the decrease in the P_s displacement. Due to the more covalent bonding of Ti with the four adjacent oxygens (O2) in the *ab* plane (*dsp* hybridization), the linkage of O1–Ti–O1 along the *c* axis becomes more flexible than the

Table 1 Crystal structures at room temperature, the T_C, P_s and CTE of PT, $P_{92}T$, and PT_{98}

	PT	$P_{92}T$	PT_{98}
Composition (Pb : Ti)	0.9979 : 1	0.9395 : 1	1 : 0.9843
a/Å	3.8990(1)	3.9019(2)	3.8994(1)
c/Å	4.1542(1)	4.1384(3)	4.1540(1)
c/*a*	1.065	1.060	1.065
V/Å^3	63.153(2)	63.006(7)	63.163(2)
δz_{Ti}/Å	0.395(7)	0.368(8)	0.400(9)
δz_{Pb}/Å	0.523(4)	0.497(4)	0.524(4)
P_s/μC cm^{-2}	66.6(9)	62.7(10)	67.1(11)
T_C/°C	490.6	484.3	491.3
CTE/°C^{-1}	-1.99×10^{-5}	-1.68×10^{-5}	-2.00×10^{-5}

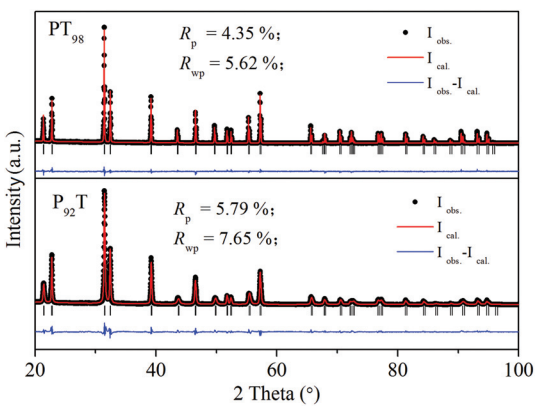

Fig. 1 XRD patterns of PT_{98} and $P_{92}T$. Observed (point), calculated (line) and difference profiles at room temperature after Rietveld refinement using the *P4mm* space group for PT_{98} and $P_{92}T$.

stiff Ti–O2 bonds[24,25] during compression and elongation. On the other hand, for the B-site deficiency, the crystal structure properties of PT are rarely affected due to the fact that only a small concentration of B-site vacancies can be introduced. Therefore, the ferroelectric properties cannot be significantly affected, and thus the NTE does not change apparently.

High temperature X-ray diffraction measurements from RT to 700 °C were performed to determine the evolution of the cell parameters of PT, $P_{92}T$ and PT_{98}. As shown in Fig. 2(a), the *a* axis in all three compositions increases upon heating, while the *c* axis decreases with increasing temperature below T_C. The *c* axis of $P_{92}T$ is also smaller than that of the other two compositions, which reduces the unit cell volume (Fig. 2b). As a result, the NTE of $P_{92}T$ is weakened significantly, while the NTE of PT_{98} is nearly identical to that of PT. The CTE of $P_{92}T$ is -1.58×10^{-5} per °C, which is smaller than that for PT (-1.99×10^{-5} per °C). As shown in Fig. 2b, the difference in the NTE is mainly due to the change in the *c*-axis. It has been known that there is coupling between the *c*-axis and P_s for PT-based ferroelectrics. In the $P_{92}T$ sample, the P_s displacements are reduced at both A and B-sites compared with PT, but not for PT_{98} (Table 1), thus indicating that ferroelectricity is reduced significantly in $P_{92}T$. It is therefore possible to conclude that the weakened NTE of $P_{92}T$ is a result of the reduction in ferroelectricity. The present study is in good agreement with previous studies.[1]

Additionally, the phase transition temperatures from tetragonal to cubic have been measured using DSC measurements as shown in Fig. 3. The T_C values of PT, $P_{92}T$ and PT_{98} are determined to be 490.6 °C, 491.3 °C and 484.3 °C, respectively. The reduction in T_C indicates a reduced P_s, which is consistent with the structure refinement results.

The Raman spectra of PT, PT_{98} and $P_{92}T$ are shown in Fig. 4. PT has a tetragonal space group symmetry C_{4v}^1 with an ABO_3 formula unit cell, and is composed of 12 optical modes that can be divided into three categories: three A_1-symmetry modes, eight *E*-symmetry modes, and one B_1-symmetry mode. The three transverse optical (TO) modes of A_1-symmetry (A_1(1TO), A_1(2TO), and A_1(3TO)) are important for $PbTiO_3$-based ferroelectric compounds because the vibrations are along the direction of the P_s.[26] Specifically, the A_1(1TO) soft mode is composed of the displacement of the TiO_6 octahedron relative to the lead atoms, while the A_1(2TO) soft mode is com-

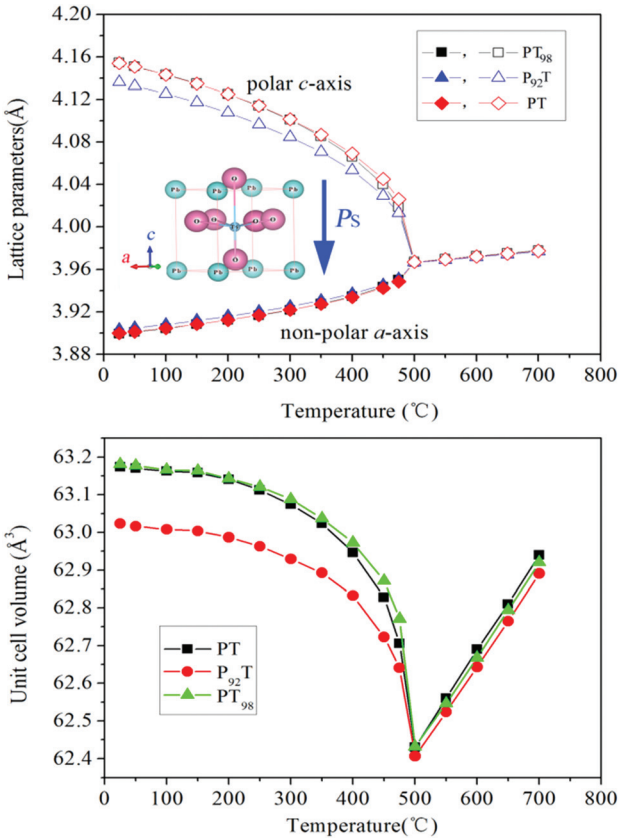

Fig. 2 Temperature dependence of the (a) lattice constant, and (b) unit cell volume of PT, $P_{92}T$ and PT_{98}. The error bar is too small to view as it is smaller than the experimental data icon.

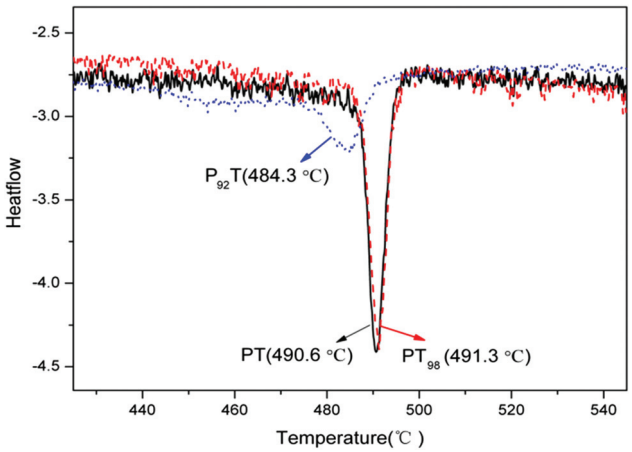

Fig. 3 DSC curves of PT, $P_{92}T$ and PT_{98} from 425 °C to 545 °C.

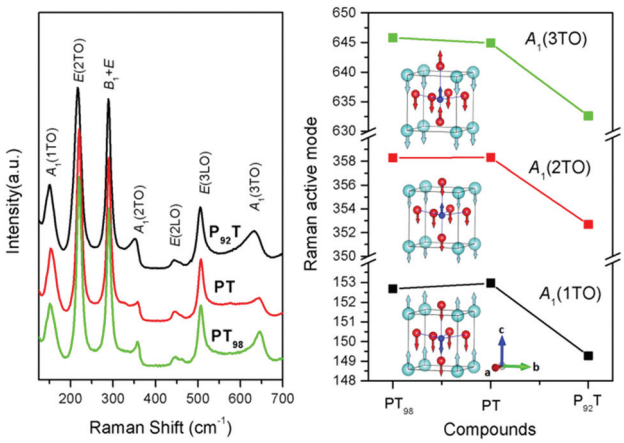

Fig. 4 (a) Raman spectra and (b) Raman active modes of PT, $P_{92}T$ and PT_{98} at room temperature.

posed of the displacements of the titanium ion relative to the oxygen and lead ions. In A_1(3TO) soft mode, titanium ions, with oxygen ions lying inbetween, move in the *c*-axis direction.[26,27] The change in these A_1-symmetry modes are highly correlative with the P_s. The results show that the Raman active modes of A_1(1TO), A_1(2TO) and A_1(3TO) soften from PT to $P_{92}T$, but remain relatively similar from PT to PT_{98} (Fig. 4). This indicates that the P_s displacements are reduced at both the A- and B-sites in $P_{92}T$, but not in PT_{98}. Furthermore, the ferroelectricity is reduced in $P_{92}T$, but not in PT_{98}, which confirms the results described above.

In view of these findings, we can thus conclude that the decrease in the P_s displacement is caused by the defects in PT. To clarify, the *c* axis is closely related with P_s displacement such that the decrease of P_s displacement triggers the decrease in the *c* axis. As shown in Table 1, both δz_{Ti} and δz_{Pb} of $P_{92}T$ are smaller than those for PT at room temperature. This is why the *c* axis of $P_{92}T$ is much smaller than that of PT; on the other hand, the *a* axis is related with the TiO_6 octahedron which is stable in a single phase, so the change in the *a* axis is small. This explains why the unit cell volume of $P_{92}T$ is smaller than that of PT in the ferroelectric phase below T_C (Fig. 2(b)). Furthermore, at T_C, the ferroelectric phase transforms to a paraelectric cubic one and the P_s displacements disappear, making the unit cell volume at T_C similar for both PT and $P_{92}T$, thus causing the NTE of $P_{92}T$ to clearly decrease. In addition, the T_C of $P_{92}T$ is found to be smaller than that of PT due to the small P_s displacement of $P_{92}T$ and less energy is needed for the phase transition, which can be described by the Landau theory.[28]

Conclusions

In summary, we studied the cation deficiency effect on negative thermal expansion in $PbTiO_3$. The resulting structural refinements and softening of A1(TO) modes suggest that Pb^{2+} deficiency in PT leads to a P_s displacement reduction and a slight decrease of T_C. As a result, the NTE is weakened from -1.99×10^{-5} per °C to -1.68×10^{-5} per °C. However, due to the limited concentration of B-site vacancies, the Ti^{4+} deficient sample does not show apparent changes in P_s displacement and CTE. The present study provides further evidence to support our previous finding that the NTE of PT-based compounds has a close relationship with P_s displacement. Our experimental result provides a possible method to control the NTE of PT-based compounds and other NTE materials by the introduction of a deficiency.

Acknowledgements

This work was supported by the National Natural Science Foundation of China (grant no. 91022016, 91422301, and 21231001), the Program for Changjiang Scholars and the Innovative Research Team in University (IRT1207), and the Fundamental Research Funds for the Central Universities, China (grant no. FRF-SD-13-008A).

Notes and references

1 F. A. Hummel, *J. Am. Ceram. Soc.*, 1951, **34**, 235.
2 G. Shirane, S. Hoshino and K. Suzuki, *Phys. Rev.*, 1950, **80**, 1150.
3 T. A. Mary, J. S. O. Evans, T. Vogt and A. W. Sleight, *Science*, 1996, **272**, 90.
4 J. Chen, J. L. Hu, J. X. Deng and X. R. Xing, *Chem. Soc. Rev.*, 2015, **44**, 3522.
5 A. W. Sleight, *Inorg. Chem.*, 1998, **37**, 2854.
6 J. S. O. Evans, *J. Chem. Soc., Dalton Trans.*, 1999, 3317.
7 P. Mohn, *Nature*, 1999, **400**, 18.
8 S. Margadonna, K. Prassides and A. N. Fitch, *J. Am. Chem. Soc.*, 2004, **126**, 15390.
9 A. Sleight, *Nature*, 2003, **425**, 674.
10 R. Roy, D. K. Agrawal and H. A. McKinstry, *Annu. Rev. Mater. Sci.*, 1989, **19**, 59.
11 Y. K. Kwon, S. Berber and D. Tománek, *Phys. Rev. Lett.*, 2004, **92**, 015901–015901.
12 J. Arvanitidis, K. Papagelis, S. Margadonna, K. Prassides and A. N. Fitch, *Nature*, 2003, **425**, 599.
13 A. L. Goodwin and C. J. Kepert, *Phys. Rev. B: Condens. Matter*, 2005, **71**, 140301–140301.
14 J. Chen, X. R. Xing, R. B. Yu and G. R. Liu, *J. Am. Ceram. Soc.*, 2005, **88**, 1356.
15 X. R. Xing, J. X. Deng, J. Chen and G. R. Liu, *Rare Met.*, 2003, **20**, 4.
16 X. R. Xing, J. Chen, J. X. Deng and G. R. Liu, *J. Alloys Compd.*, 2004, **360**, 286.
17 D. Taylor, *Br. Ceram. Trans. J.*, 1985, **84**, 181.
18 J. Chen, X. R. Xing, C. Sun, P. Hu, R. B. Yu, X. W. Wang and L. H. Li, *J. Am. Chem. Soc.*, 2008, **130**, 1144.
19 P. Hu, J. Chen, J. X. Deng and X. R. Xing, *J. Am. Chem. Soc.*, 2010, **132**, 1925.
20 J. Chen, X. R. Xing, G. R. Liu, J. H. Li and Y. T. Liu, *Appl. Phys. Lett.*, 2006, **89**, 101914.
21 J. Chen, X. R. Xing, R. B. Yu and G. R. Liu, *Appl. Phys. Lett.*, 2005, **87**, 231915.
22 C. Sun, Z. M. Cao, J. Chen, R. B. Yu, X. Y. Sun, P. H. Hu, G. R. Liu and X. R. Xing, *Phys. Status Solidi B*, 2008, **245**, 11.
23 J. Chen, K. Nittala, J. S. Forrester, J. L. Jones, J. X. Deng, R. B. Yu and X. R. Xing, *J. Am. Chem. Soc.*, 2011, **133**, 11144.
24 R. E. Cohen, *Nature*, 1992, **358**, 136–138.
25 Y. Kuroiwa, S. Aoyagi, A. Sawada, J. Harada, E. Nishibori, M. Takata and M. Sakata, *Phys. Rev. Lett.*, 2001, **87**, 217601.
26 J. D. Freire and R. S. Katiyar, *Phys. Rev. B: Condens. Matter.*, 1988, **37**, 2074–2085.
27 J. Frantti, V. Lantto, S. Nishio and M. Kakihana, *Phys. Rev. B: Condens. Matter.*, 1999, **59**, 12.
28 R. A. Cowley, *Adv. Phys.*, 1980, **29**, 1.

